nature portfolio

https://doi.org/10.1038/s41596-023-00822-x

Supplementary information

Graphene–molecule–graphene single-molecule junctions to detect electronic reactions at the molecular scale

In the format provided by the authors and unedited

Supplementary Information

Table of Contents

1. Comparison with other single-molecule approaches

Optical methods are suitable for measuring fluorescent molecules or require fluorescent labelling (associated to this one needs to consider its spatial size (about 1 nm), quantum yield (> 20 %), excited state lifetime (< 5 ns), photobleaching (stability), blinking, spectral shifts[1,2]), and provide rich nanoscopic information by characterising the intensity (usually depending on the gain of the camera) variations of the fluorescence[4] and emission spectrum[3] (usually 400−800 nm). The traditional optical microscopy is limited by the diffraction limit of light and provides an image of the microstructure with about 200 nm resolution. The characterisation with single-molecule resolution was realised by the development of a super high-resolution microscopy including the hardware structure[4,5] and imaging algorithm[6]. In addition, the time resolution is also important, which depends on the exposure time (about milliseconds). This optical approach is suitable for the studies of conformational changes of biomacromolecules[2] and enzymatic reactions[7].

Chain-like molecules (such as polymers, DNA, and RNA) provide an effective interface to conduct mechanical analysis. Through the attachment of one terminal via magnetic[8]/optical tweezers[9], the monitored force (pN scale[8]) or movement (nm scale[8]) of the other terminal can be attributed to the dynamic behavior of the chain including polymerisation, twining, and folding. In addition, the intermolecular affinity properties can be characterised by a conductive atomic force microscope (AFM)[10–13].

Electrical approaches provide more structure-related information with higher temporal resolution (about microseconds), in particular for small molecules. The molecule translocating in the nanopore can be detected by the blockade in the ionic current that is produced during translocation. The classical example is the fast readout of the DNA sequence as it threads through the nanopore[14,15]. The current resolution mainly depends on the relative size of the nanopore diameter and the molecule as well as the applied voltage. The single-molecule junction (i.e. the nanogap) provides a closer relationship between the structure and electronic properties owing to the molecule being the dominant conductive channel[16–19]. The detailed comparison among the single-molecule junctions is provided in the main text.

2. Schematic of the device preparation.

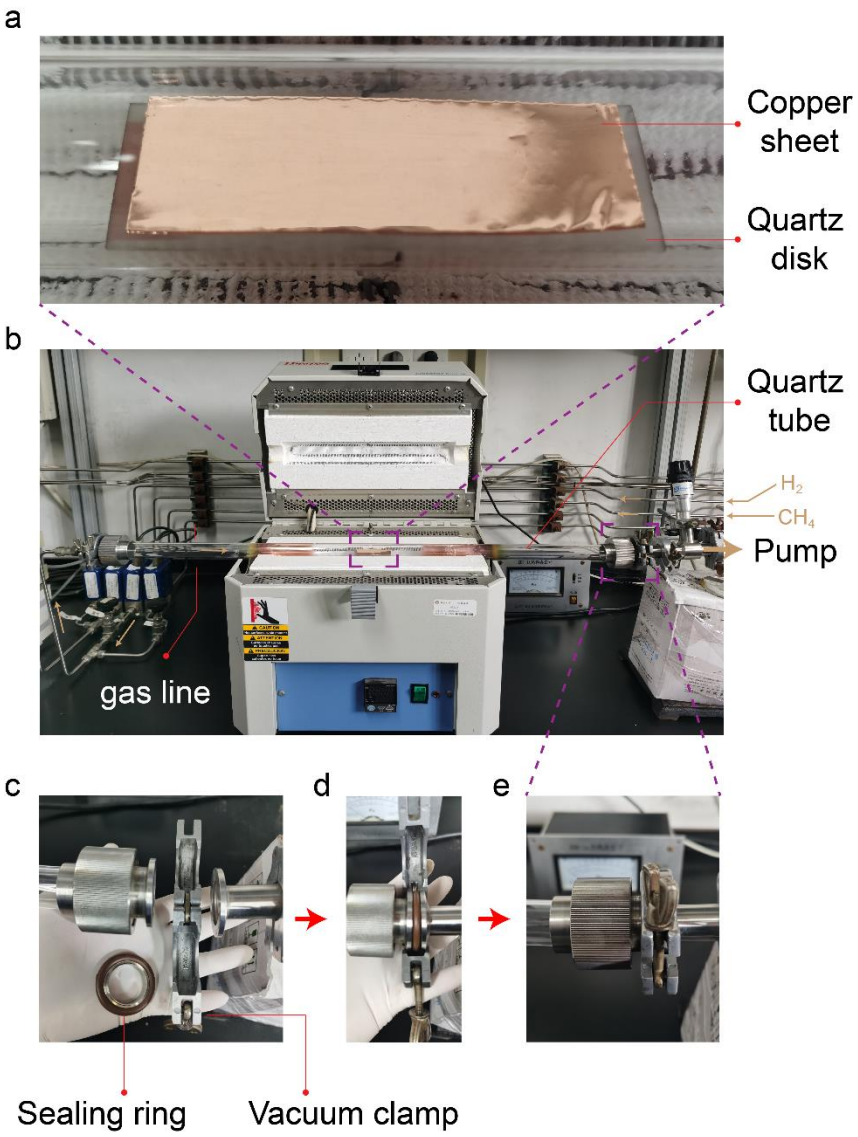

Figure S1 | Schematic of the system for graphene growth on copper sheets. a. The enlarged image of the copper sheet in the quartz tube of the furnace (**b**). The copper sheet was supported by the quartz disk. **b**. Schematic of the whole system, including the gas source (from the H_2 and CH_4 cylinders on the balcony), the gas line, the quartz tube with the corresponding sealing interface, the tube furnace, and the oil pump. **c**–**e**. Schematic of sealing the system. The tube in the quartz furnace was detachably connected to the oil pump with a vacuum clamp and a vacuum sealing ring.

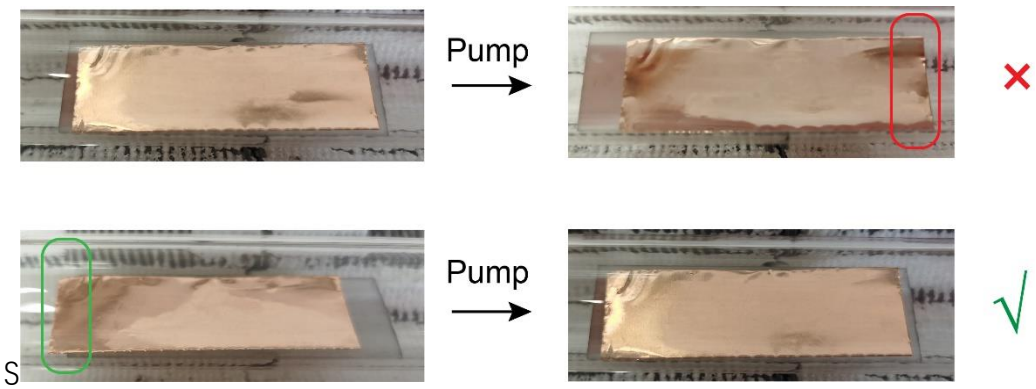

Figure S2 | Schematic of loading a copper sheet on the quartz tube. A moderate deviation of the copper sheet to the quartz disk could compensate its migration from the flow air during pumping.

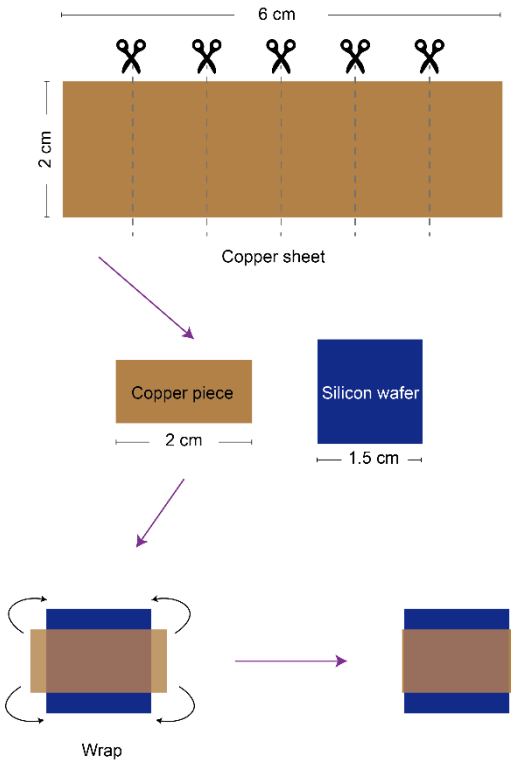

Figure S3 | Schematic of wrapping the copper piece on the silicon wafer for subsequent spin coating.

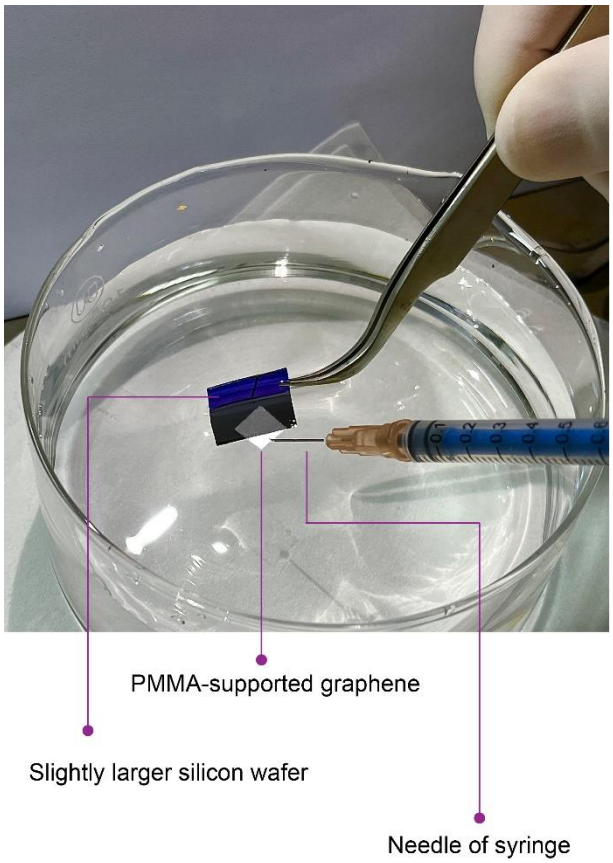

Figure S4 | Schematic of using a needle to assist in picking up the PMMA-supported graphene.

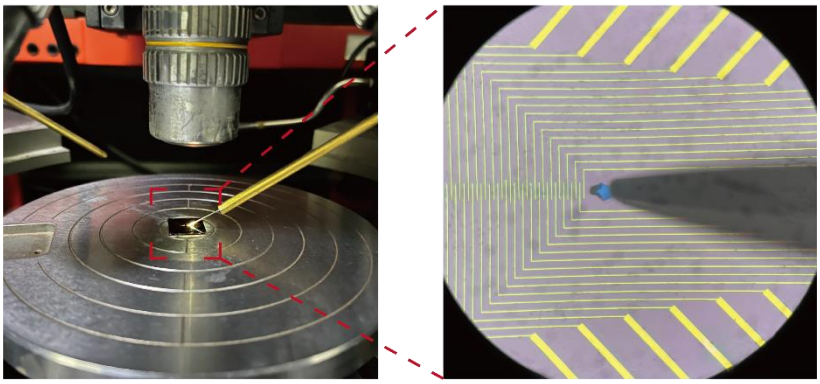

Figure S5 | Schematic of poking a hole in the PMMA layer near the end of the graphene ribbon by using a needle tip.

3. Characterisation of the sample/device.

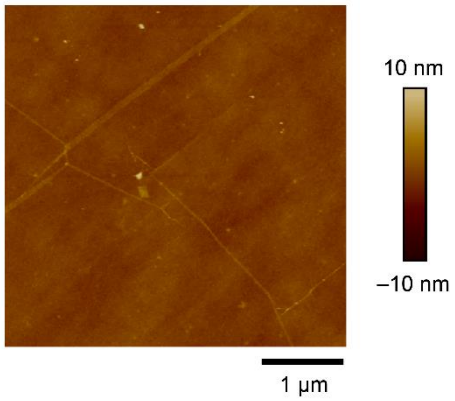

Figure S6 | The AFM image of the graphene in the FET.

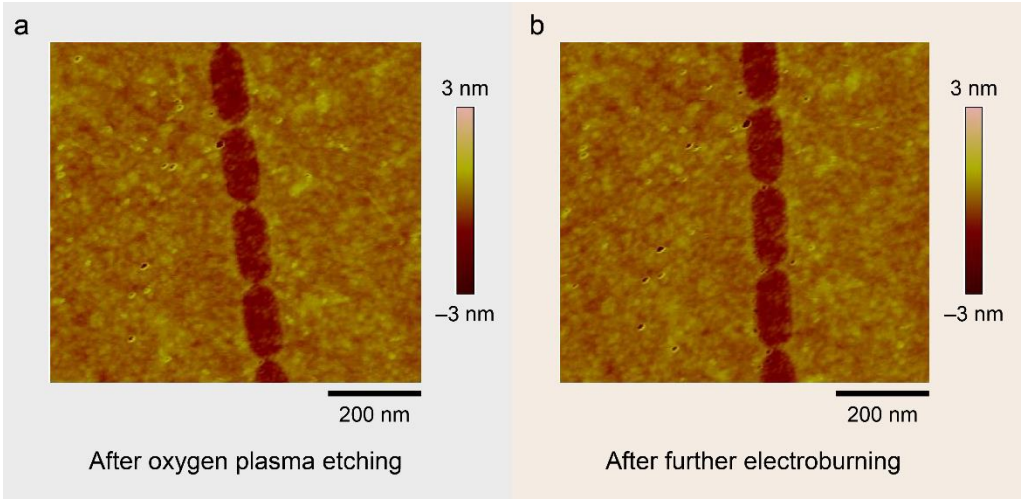

Figure S7 | The high-resolution AFM images of an electrode pair array after oxygen plasma etching (a) and after further electroburning (b), respectively.

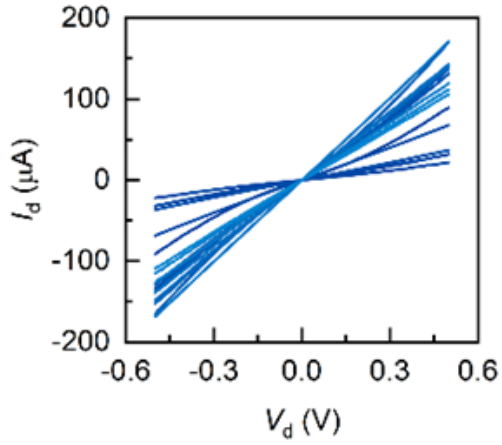

Figure S8 | Typical *I–V* curves of incompletely cut devices.

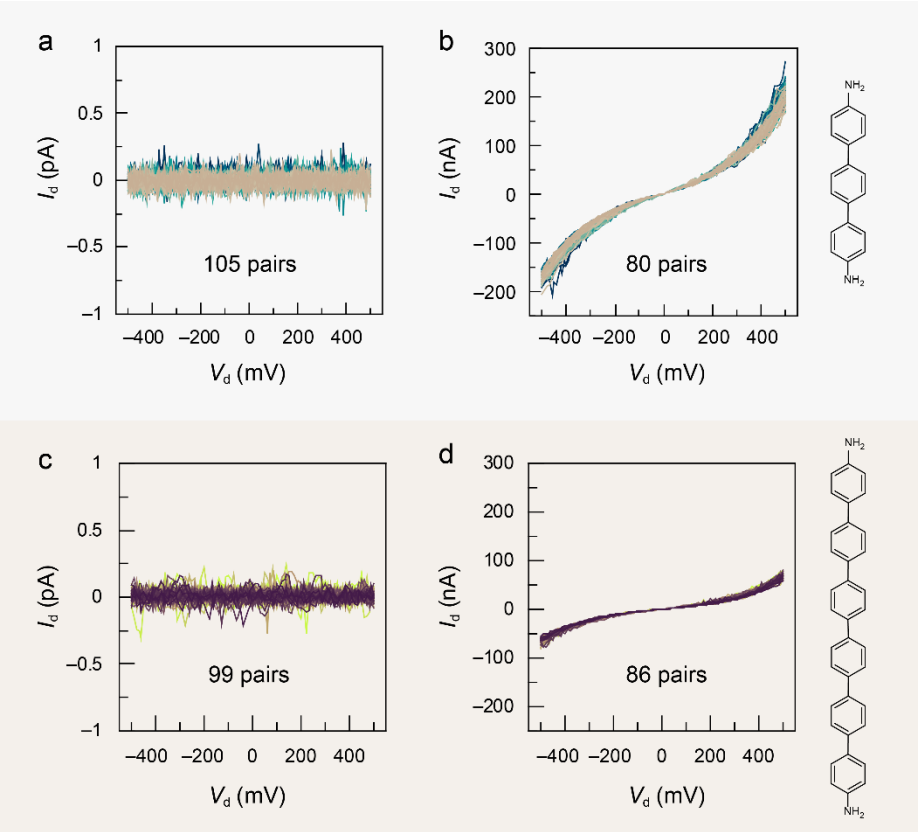

Figure S9 | *I–V* curves of 185 pairs of Au electrodes on two chips which integrated two kinds of molecules, respectively. 105-pairs unsuccessful connection (**a**) and 80-pairs successful connection of triphenyl molecular bridges (**b**) were obtained on one chip. 99-pairs unsuccessful connection (**c**) and 86-pairs successful connection of hexaphenyl molecular bridges (**d**) were obtained on the other chip.

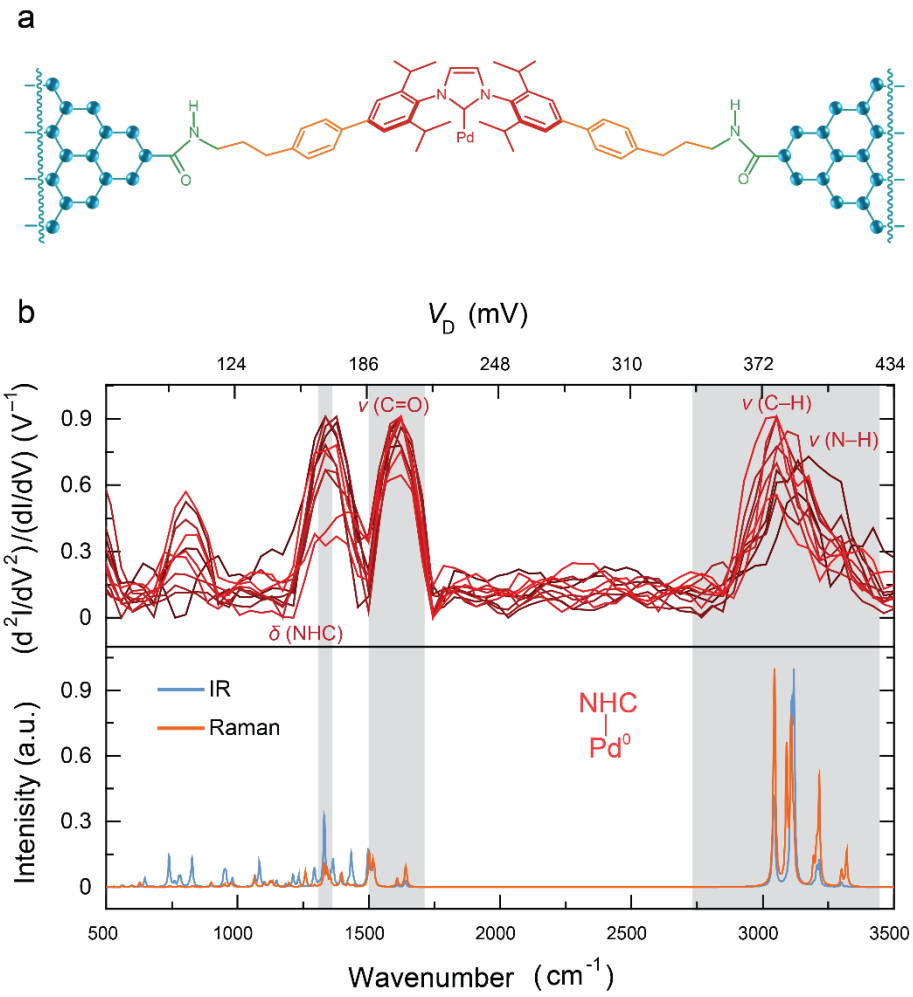

Figure S10 | Inelastic electron tunneling spectra (IETS) of the Pd(0) catalyst integrated between graphene electrodes[20]. a. Schematic of the molecular structure. **b.** The corresponding measured IETS and the calculated infrared and Raman spectra of the functional centre. The devices, which were further used to study the physical properties and chemical reactions, were characterised by IETS firstly. The data of 11 different devices were displayed here and all of them showed the target single-molecule signatures. The peaks of δ(NHC) (~167 mV), ν(C−H) (~389 mV), ν(C=O) (~200 mV), and ν(N−H) (~400 mV) were marked, indicating that the intrinsic vibrations of the Pd(0) catalyst are measurable at all the devices.

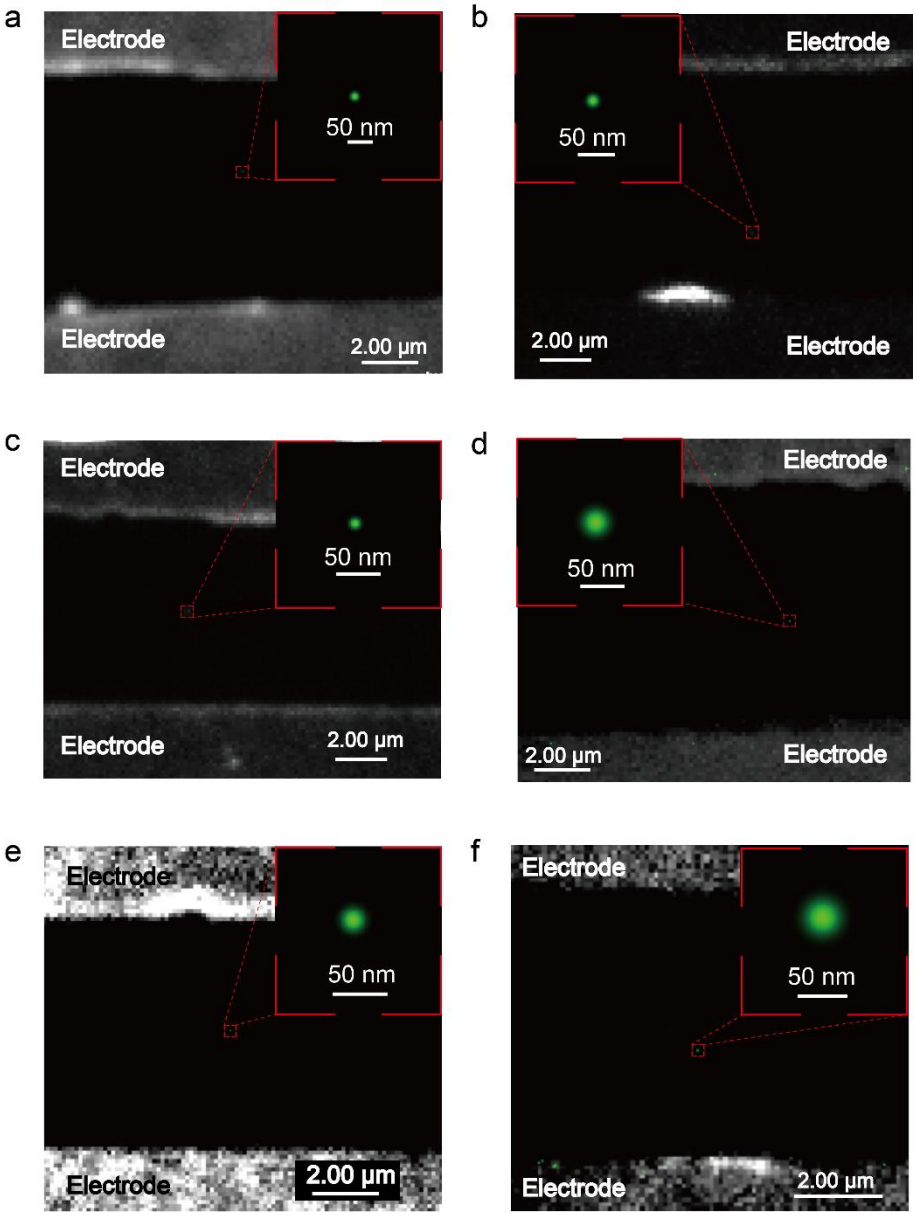

Figure S11 | Super high-resolution images of 6 different single-maleimide devices[21]. The devices, which were further used to study the physical properties and chemical reactions, were characterised by STORM firstly. All the measured 6 devices (**a**–**f**) showed only one-molecule integration between metal electrodes.

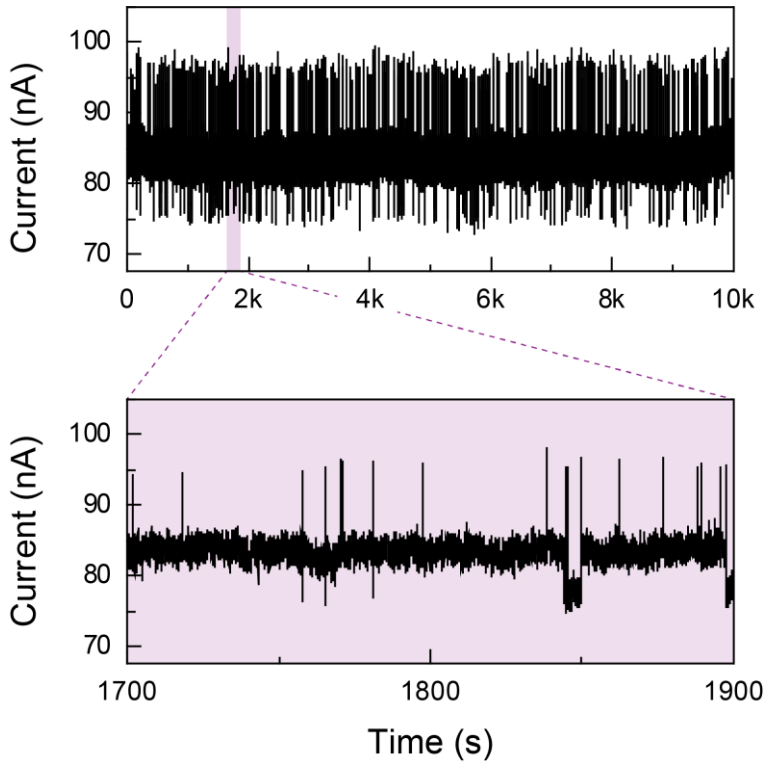

Figure S12 | Long-term monitoring of the Claisen rearrangement at 0.5 V via integrating a molecular bridge with allyl phenyl ether centre into graphene electrodes[22].

References

1. Ha, T. & Tinnefeld, P. Photophysics of fluorescent probes for single-molecule biophysics and super-resolution imaging. *Annu. Rev. Phys. Chem.* **63**, 595−617 (2012).
2. Verbrugge, S., Lansky, Z. & Peterman, E. J. G. Kinesin's step dissected with single-motor FRET. *Proc. Natl. Acad. Sci. USA* **106**, 17741−17746 (2009).
3. Eid, J. *et al.* Real-time DNA sequencing from single polymerase molecules. *Science* **323**, 133−138 (2009).
4. Klar, T. A., Jakobs, S., Dyba, M., Egner, A. & Hell, S. W. Fluorescence microscopy with diffraction resolution barrier broken by stimulated emission. *Proc. Natl. Acad. Sci. USA* **97**, 8206−8210 (2000).
5. Hell, S. W. Far-field optical nanoscopy. *Science* **316**, 1153−1158 (2007).
6. Rust, M. J., Bates, M. & Zhuang, X. Sub-diffraction-limit imaging by stochastic optical reconstruction microscopy (STORM). *Nat. Methods* **3**, 793−795 (2006).
7. Lu, H. P., Xun, L. & Xie, X. S. Single-molecule enzymatic dynamics. *Science* **282**, 1877−1882 (1998).
8. Liu, C. et al. Single polymer growth dynamics. *Science* **358**, 352−355 (2017).
9. Heller, I., Hoekstra, T. P., King, G. A., Peterman, E. J. G. & Wuite, G. J. L. Optical tweezers analysis of DNA-protein complexes. *Chem. Rev.* **114**, 3087−3119 (2014).
10. Florin, E. L., Moy, V. T. & Gaub, H. E. Adhesion forces between individual ligand-receptor pairs. *Science* **264**, 415−417 (1994).
11. Huang, W. et al. Maleimide-thiol adducts stabilized through stretching. *Nat. Chem.* **11**, 310−319 (2019).
12. Sluysmans, D., Devaux, F., Bruns, C. J., Stoddart, J. F. & Duwez, A. S. Dynamic force spectroscopy of synthetic oligorotaxane foldamers. *Proc.*

Natl. Acad. Sci. USA **115**, 9362−9366 (2018).

13. Lussis, P. et al. A single synthetic small molecule that generates force against a load. *Nat. Nanotechnol.* **6**, 553−557, (2011).
14. Venkatesan, B. M. & Bashir, R. Nanopore sensors for nucleic acid analysis. *Nat. Nanotechnol.* **6**, 615−624 (2011).
15. Heerema, S. J. & Dekker, C. Graphene nanodevices for DNA sequencing. *Nat. Nanotechnol.* **11**, 127−136 (2016).
16. Derosa, P. A. & Seminario, J. M. Electron transport through single molecules: Scattering treatment using density functional and green function theories. *J. Phys. Chem. B* **105**, 471−481 (2001).
17. Metzger, R. M. Unimolecular electronics. *Chem. Rev.* **115**, 5056−5115 (2015).
18. Cuevas, J. C. & Scheer, E. *Molecular electronics: An introduction to theory and experiment*. (World Scientific, 2010).
19. Di Ventra, M. *Electrical transport in nanoscale systems*. (Cambridge University Press, 2008).
20. Yang, C. et al. Unveiling the full reaction path of the Suzuki–Miyaura cross-coupling in a single-molecule junction. *Nat. Nanotechnol.* **16**, 1214−1223 (2021).
21. Yang, C. et al. Electric field-catalyzed single-molecule Diels-Alder reaction dynamics. *Sci. Adv.* **7**, eabf0689 (2021).
22. Guo, Y. et al. Accurate single-molecule kinetic isotope effects. *J. Am. Chem. Soc.* **144**, 3146−3153 (2022).